Eur. Phys. J. A **25**, s01, 499–502 (2005)
DOI: 10.1140/epjad/i2005-06-032-2

EPJ A direct
electronic only

Shell-model description of neutron-rich pf-shell nuclei with a new effective interaction GXPF1

M. Honma[1,a], T. Otsuka[2,3], B.A. Brown[4], and T. Mizusaki[5]

[1] Center for Mathematical Sciences, University of Aizu, Tsuruga, Ikki-machi, Aizu-Wakamatsu, Fukushima 965-8580, Japan
[2] Department of Physics and Center for Nuclear Study, University of Tokyo, Hongo, Tokyo 113-0033, Japan
[3] RIKEN, Hirosawa, Wako-shi, Saitama 351-0198, Japan
[4] National Superconducting Cyclotron Laboratory and Department of Physics and Astronomy, Michigan State University, East Lansing, MI 48824-1321, USA
[5] Institute of Natural Sciences, Senshu University, Higashimita, Tama, Kawasaki, Kanagawa 214-8580, Japan

Received: 1 October 2004 /
Published online: 22 April 2005 –

Abstract. The shell-model effective interaction GXPF1 is tested for the description of unstable pf-shell nuclei. The GXPF1 successfully describes the $N = 32$ shell gap in Ca, Ti and Cr isotopes, while the deviation of predicted $E_x(2_1^+)$ in ^{56}Ti from the recent experimental data requires the modification of the Hamiltonian especially in the $T = 1$ matrix elements related to the $p_{1/2}$ and $f_{5/2}$ orbits. The modified interaction gives improved description simultaneously for all these isotope chains.

PACS. 21.60.Cs Shell model – 21.30.Fe Forces in hadronic systems and effective interactions

1 Introduction

The nuclear shell model has been one of the most powerful tools for the microscopic study of the nuclear structure. Owing to recent developments in computational facilities as well as numerical methods, most of the pf-shell nuclei are now in the scope of exact or nearly exact $0\hbar\omega$ calculations. The success of the shell model crucially depends on the choice of the effective interaction, however.

For practical use in a wide region of the pf-shell, we have recently derived an effective interaction GXPF1 [1]. Starting from the microscopic effective interaction [2] derived from the Bonn-C potential (it is simply referred as G hereafter), we modified 70 well-determined linear combinations of 4 single-particle energies and 195 two-body matrix elements by iterative fitting calculations to about 700 experimental energy data out of 87 nuclei.

The GXPF1 interaction was tested [3] extensively from various viewpoints such as binding energies, electormagnetic moments, energy-levels and transitions, revealing its predictive power in the wide region of the pf-shell. At the same time, it was found that the deviation of the shell-model prediction from available experimental data appeared to be sizable in binding energies of $N \geq 35$ nuclei and in magnetic moments of $Z \geq 32$ even-even nuclei. This observation suggests the limitation of its applicability near the end of the pf-shell.

Since the GXPF1 was determined by using the experimental energy data mainly of stable nuclei, it is a challenging test to apply this interaction to describe/predict the structure of unstable nuclei. Recent data of such unstable nuclei may provide crucial information for clarifying possible problems in some parts of the effective interaction.

This paper is organized as follows: In sect. 2, we clarify the problem in GXPF1 revealed by new experimental data of neutron-rich nuclei around Ti isotopes. In sect. 3, we investigate possible modifications of GXPF1 so as to improve the description, and the validity of such modifications is examined. Several results obtained with the modified interaction are presented in sect. 4.

The shell-model calculations were carried out by using the code MSHELL [4]. We also consider the KB3G [5] interaction as a reference, because it gives an excellent description for light pf-shell nuclei ($A \leq 52$). The KB3G interaction is the latest version of the family of the KB3 [6] interaction. Both GXPF1 and KB3G predict similar structure for light stable nuclei, but they give rather different results in several cases of neutron-rich nuclei.

2 Shell evolution

One of the interesting results obtained by the GXPF1 for the neutron-rich nuclei is the shell evolution, *i.e.*, the change of the shell structure due to the occupation of single-particle orbits. Figure 1 shows the excitation energies $E_x(2_1^+)$ for Ca, Ti and Cr isotopes as a function of

[a] Conference presenter; e-mail: m-honma@u-aizu.ac.jp

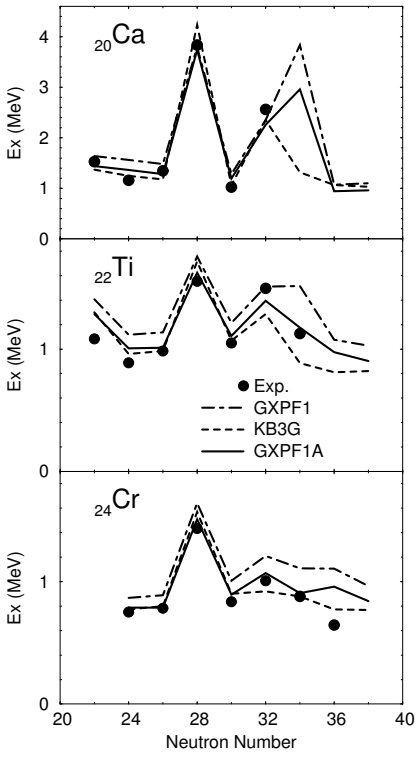

Fig. 1. Systematics of $E_x(2_1^+)$ for even-even Ca, Ti, and Cr isotopes. Experimental data (closed circles) are compared to shell-model results obtained with three effective interactions: GXPF1 (dod-dashed line), KB3G (dashed line) and GXPF1A (solid line). Experimental data are taken from refs. [7,8,9,10].

the neutron number N. It can be seen that the GXPF1 successfully describes the variation of E_x for all these isotope chains, including the increase of E_x at $N = 28$ shell closure. In addition, one can find a remarkable increase in E_x from $N = 30$ to 32 for all these isotopes, which has been interpreted as an indication of another shell closure. Since the experimental energy data included in the fitting calculations for the derivation of GXPF1 were limited to $N \leq 31$, 30 and 32 for Ca, Ti and Cr, respectively, it turns out that the prediction for E_x of ^{54}Ti was in good agreement with the experiment [9].

In order to illustrate the shell evolution, it is useful to consider the effective single-particle energy (ESPE) for pf-shell nuclei [1]. The ESPE contains the effects of both bare single-particle energy and the angular-momentum averaged two-body interaction. We focus on the behavior of the $p_{1/2}$ and $f_{5/2}$ orbits relative to the $p_{3/2}$ orbit as a function of N, which is shown in fig. 2 for even-even Ca, Ti and Cr isotopes.

The $N = 32$ shell gap is a result of the large spin-orbit splitting between the $p_{3/2}$ and $p_{1/2}$ orbits. In fact, as seen in fig. 2, both GXPF1 and KB3G predict no single-particle orbit between these two orbits, which are separated by about 2 MeV in Ca and Ti. The shell gap disappears as more and more protons are added in the $f_{7/2}$ orbit, because the neutron $f_{5/2}$ orbit rapidly comes down well below the $p_{1/2}$ orbit due to the large attractive proton-

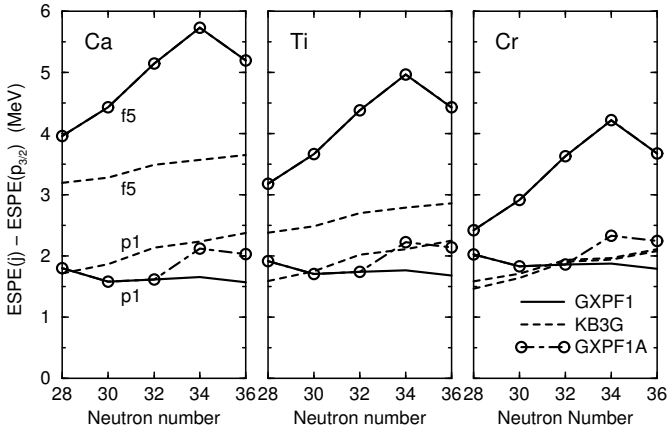

Fig. 2. Effective single-particle energies of the neutron $p_{1/2}$ and $f_{5/2}$ orbits relative to the $p_{3/2}$ orbit calculated by three effective interactions: GXPF1 (solid lines), KB3G (dashed lines) and GXPF1A (dot-dashed lines).

neutron interaction between the member of the spin-orbit partner $j_>$-$j_<$ [11]. As for Cr, GXPF1 predicts that the $f_{5/2}$ orbit is still higher than the $p_{1/2}$ orbit by 1.5 MeV and there exists a corresponding increase in E_x at $N = 32$. On the other hand, KB3G produces almost degenerate $f_{5/2}$ and $p_{1/2}$ orbits, and accordingly, the increase of E_x can hardly be seen. Nevertheless, the formation mechanism of $N = 32$ shell gap is robust and the jump of $E_x(2_1^+)$ at $N = 32$ is, at least qualitatively, predicted by various effective interactions such as KB3, KB3G and FPD6 [12].

In addition to $N = 32$, GXPF1 predicts another increase in E_x at $N = 34$ for Ca and Ti, which is attributed to the large energy gap between the neutron $f_{5/2}$ and $p_{1/2}$ orbits [11]. However, in the recent experiment for ^{56}Ti [10], it turned out that the measured $E_x(2_1^+)$ is lower than the GXPF1 prediction by 0.4 MeV, indicating a problem of GXPF1 for the description of neutron-rich nuclei. In contrast with the $N = 32$ shell gap, the persistence of the shell gap with $N > 32$ and $Z > 20$ is more complex: it is predicted by GXPF1 and KB3, while not by FPD6 and KB3G. It can be seen in fig. 2 that, in the case of Ti, the difference of the ESPE between the $f_{5/2}$ and $p_{1/2}$ orbits at $N = 34$ is only 0.7 MeV in KB3G, while it is 3.2 MeV in GXPF1. This gap is already about 1.3 MeV at $N = 28$ and rapidly increases toward $N = 34$. Since the N-dependence of the $p_{1/2}$ orbit is modest in both interactions, the behavior of the $f_{5/2}$ orbit is of great interest.

3 Modification of GXPF1

In order to improve the description of $E_x(2^+)$ for ^{56}Ti, one possible choice is to lower the single particle energy of the $f_{5/2}$ orbit by 0.8 MeV, as suggested in ref. [10]. In fact it remedies this discrepancy by about 0.2 MeV. However, such a modification affects the description of other neighboring nuclei. For example, in fig. 3, energy levels of ^{54}Ti are compared with experimental data including high-spin states. One can find that the correspondence between

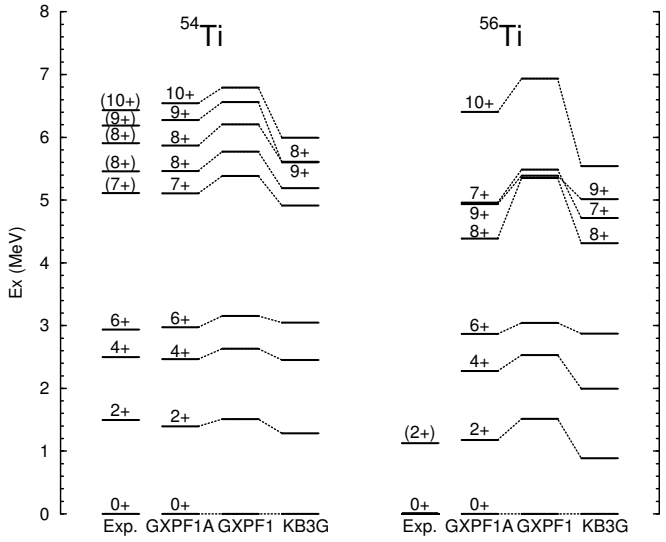

Fig. 3. Energy levels of ^{54,56}Ti. Experimental data [9,10] are compared to shell-model results with three effective interactions GXPF1, KB3G and GXPF1A.

the experimental data and the GXPF1 prediction is very good. It was argued in ref. [9] that the energy gap above the yrast 6^+ state is one evidence of the $N = 32$ shell closure. In the shell model results, the leading configuration of 7^+_1 and 8^+_1 states is $\pi f^2_{7/2}\nu f^8_{7/2}p^3_{3/2}p^1_{1/2}$, while it is $\pi f^2_{7/2}\nu f^8_{7/2}p^3_{3/2}f^1_{5/2}$ for 9^+_1 and 10^+_1. The lowering of the $f_{5/2}$ orbit affects only the latter two states, giving rise to worse agreement between the shell model results and the experimental data. It is also the case for high-spin states in ^{53}Ti [13], suggesting that the ESPE for the $p_{3/2}$ and $f_{5/2}$ orbits predicted by GXPF1 is reasonable at least near $N = 32$. Therefore, we search for another way to solve the problem in ^{56}Ti. Since the experimental data included in the derivation of GXPF1 were limited to $Z \leq 32$, it is natural to anticipate that there remains relatively large uncertainty in the matrix elements which are related to the $p_{1/2}$ and $f_{5/2}$ orbits.

It can be seen in fig. 1 that GXPF1 predicts slightly higher $E_x(2^+)$ than experimental data commonly for almost all nuclei. This is naturally understood by recalling that we have adopted the few-dimensional-bases approximation (FDA) [14] for deriving GXPF1 in order to obtain shell-model wave functions for all states included in the fit. Since the FDA wave function is a superposition of several angular-momentum projected Slater determinants, the pairing correlations cannot be described accurately. Therefore, the determined "strengths" (*i.e.* two-body matrix elements) for the pairing interaction become relatively stronger than they should be in the exact calculations. Thus we change the following pairing matrix elements to be less attractive. The increments are

$$\Delta V\left(f_{7/2}f_{7/2}f_{7/2}f_{7/2};\ J=0,\ T=1\right) = +0.2\,\mathrm{MeV}, \quad (1)$$
$$\Delta V\left(f_{5/2}f_{5/2}p_{1/2}p_{1/2};\ J=0,\ T=1\right) = +0.5\,\mathrm{MeV}, \quad (2)$$
$$\Delta V\left(p_{1/2}p_{1/2}p_{1/2}p_{1/2};\ J=0,\ T=1\right) = +0.5\,\mathrm{MeV}. \quad (3)$$

Table 1. Summary of modified two-body matrix elements $V(2j_a2j_b2j_c2j_d;JT)$ (in MeV). Those of other effective interactions are also shown for comparison.

V	GXPF1	GXPF1A	G	KB3G
$V(7777;01)$	-2.439	-2.239	-2.045	-1.920
$V(5511;01)$	-0.809	-0.309	-0.450	-0.392
$V(1111;01)$	-0.447	$+0.053$	-0.308	$+0.151$
$V(5151;21)$	-0.152	-0.502	-0.174	-0.135
$V(5151;31)$	$+0.238$	$+0.488$	$+0.207$	$+0.205$

Here, we consider only these three matrix elements, because they are enough to improve the results for all nuclei discussed in the present study, and we should keep the modifications minimal. The modification (1) accounts only for the systematic error due to the FDA. On the other hand, the shift is relatively large in (2) and (3), which are related to the $p_{1/2}$ and $f_{5/2}$ orbits, allowing additional 0.3 MeV uncertainty due to the lack of data for determining these matrix elements. The modification (3) affects the monopole matrix element and therefore changes the ESPE of the $p_{1/2}$ orbit for $N > 32$, as shown in fig. 2 with dot-dashed lines. The energy gap between $f_{5/2}$ and $p_{1/2}$ is made narrower at $N = 34$ by 0.5 MeV, promoting the mixing between these orbits. Such a modification is reasonable from the viewpoint of systematics in the monopole part after the subtraction of the tensor force [15].

In ref. [3], we have pointed out that the strength of quadrupole-quadrupole (QQ) interaction $[(f_{7/2})^\dagger(\tilde{p}_{3/2})]^{(2)} \cdot [(p_{3/2})^\dagger(\tilde{f}_{7/2})]^{(2)}$ in GXPF1 is made to be much stronger than the original G as well as KB3G, leading to successful description of 2^+ states on top of the ^{56}Ni closed core. In fact, the strength of this term is -0.81, -0.38, and -0.34 MeV for GXPF1, G, and KB3G, respectively. In the case of ^{56}Ti, we can consider a $\nu f^8_{7/2}p^4_{3/2}$ core, and expect that the similar correction takes effects for lowering $E_x(2^+)$. The strength of $[(f_{5/2})^\dagger(\tilde{p}_{1/2})]^{(2)} \cdot [(p_{1/2})^\dagger(\tilde{f}_{5/2})]^{(2)}$ term is -0.23, -0.22, and -0.20 MeV for GXPF1, G, and KB3G, respectively. Then, the relevant matrix elements are changed by

$$\Delta V\left(f_{5/2}p_{1/2}f_{5/2}p_{1/2};\ J=2,\ T=1\right) = -0.35\,\mathrm{MeV}, \quad (4)$$
$$\Delta V\left(f_{5/2}p_{1/2}f_{5/2}p_{1/2};\ J=3,\ T=1\right) = +0.25\,\mathrm{MeV}. \quad (5)$$

This modification keeps the monopole centroid unchanged, and the strength of the QQ term is now -0.58 MeV.

The modified matrix elements are summarized in table 1. These modifications are typically within about 0.3 MeV in comparison with other effective interactions. This modified GXPF1 is referred to as GXPF1A hereafter.

4 Results and discussions

It can be seen in fig. 1 that GXPF1A gives better description of the systematics of $E_x(2^+)$ than GXPF1 for almost

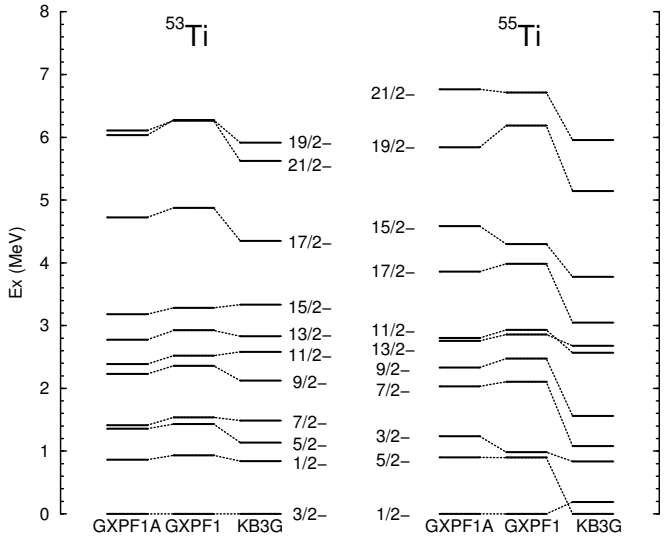

Fig. 4. Calculated energy levels of ^{53,55}Ti with three effective interactions GXPF1, KB3G and GXPF1A.

all nuclei. There still remains a large deviations from experiment in ^{60}Cr ($N = 36$), but it has been shown that a $(9/2^+)$ state appears at 503 keV in ^{59}Cr [16] and the pf-shell space is already insufficient at $N = 35$. Therefore we do not expect the accurate description for $N \geq 35$, consistently with the systematics in binding energies and electromagnetic moments mentioned before.

We have confirmed that GXPF1A improves the agreement with experimental data also for high-spin states in ^{54}Ti, as shown in fig. 3. The difference between GXPF1A and KB3G is apparent in 9^+ and 10^+ states, which can be understood as a result of the difference in the position of $f_{5/2}$ orbit (see fig. 2). As for ^{56}Ti, GXPF1A and KB3G predict very different excitation energy for 10^+ state by 0.9 MeV. The leading configuration of this state is $\pi f_{7/2}^2 \nu f_{7/2}^8 p_{3/2}^4 f_{5/2}^2$ (46% and 62% for GXPF1A and KB3G, respectively) and the difference reflects again the position of the $f_{5/2}$ orbit.

The information of the $f_{5/2}$ orbit is obtained also from odd-A nuclei. Figure 4 shows the calculated yrast energy levels of ^{53}Ti and ^{55}Ti. In ^{53}Ti, the similarity between the results of GXPF1A and KB3G can be seen for low-spin states, where the dominant configuration is $\pi f_{7/2}^2 \nu f_{7/2}^8 p_{3/2}^3$. A sizable difference appears first in $17/2^-$ state with a dominant configuration $\pi f_{7/2}^2 \nu f_{7/2}^8 p_{3/2}^2 f_{5/2}^1$. There exist remarkable differences in ^{55}Ti. The ground-state spin-parity is predicted to be $1/2^-$ by GXPF1A, while it is $5/2^-$ by KB3G. It is discussed [17] that the branching pattern of the β-decay is consistent with the ground-state spin greater than 1/2. If it is the case, the lower $f_{5/2}$ is favored. However, the arguments of 2^+ in ^{56}Cr and 10^+ in ^{54}Ti suggest higher $f_{5/2}$ than the KB3G prediction at $N = 32$. Definite assignment of the spin-parity is desired for further discussions.

Finally, we come back to $N = 34$ shell closure. In ^{54}Ca, the difference of the ESPE between the $f_{5/2}$ and $p_{1/2}$ orbits is reduced from 4.1 MeV (GXPF1) to 3.6 MeV (GXPF1A) and, correspondingly, $E_x(2^+)$ is decreased from 3.8 MeV to 3.0 MeV. Nevertheless, this excitation energy is higher than that of ^{52}Ca (2.56 MeV experimentally), suggesting the $N = 34$ shell closure in the Ca isotopes as predicted in ref. [11]. In ^{49}Ca, the single-particle strength of the neutron $p_{1/2}$ orbit is lower in energy than that of $f_{5/2}$ by about 1.8 MeV [18], which appears rather close to the predictions of GXPF1 and KB3G. The size of this energy gap is large enough to be comparable to that between the $p_{3/2}$ and $p_{1/2}$ orbits at $N = 32$. As more neutrons are put into the $p_{3/2}$ and $p_{1/2}$ orbits toward $N = 34$, this gap significantly widens in GXPF1A, while it is almost constant in KB3G. This difference is due to the $T = 1$ monopole effect. Therefore, $E_x(2^+)$ of ^{54}Ca reflects the $T = 1$ part of the monopole property. The experimental determination of $E_x(2^+)$ will provide crucial information.

5 Summary

We have considered possible modifications of GXPF1 in order to improve the description of neutron-rich pf-shell nuclei. By changing five two-body matrix elements within reasonable amount, the discrepancy between the recent experimental data and theoretical prediction in ^{56}Ti can be remedied. Therefore the problem can be attributed to uncertainties in several matrix elements which could not be well determined in the fitting calculations for deriving GXPF1 because of the insufficient data. The modified interaction still predicts an increase of $E_x(2_1^+)$ at ^{54}Ca, suggesting the appearance of the $N = 34$ shell gap in Ca isotopes.

References

1. M. Honma, T. Otsuka, B.A. Brown, T. Mizusaki, Phys. Rev. C **65**, 061301(R) (2002).
2. M. Hjorth-Jensen, T.T.S. Kuo, E. Osnes, Phys. Rep. **261**, 125 (1995).
3. M. Honma, T. Otsuka, B.A. Brown, T. Mizusaki, Phys. Rev. C **69**, 034335 (2004).
4. T. Mizusaki, RIKEN Accel. Prog. Rep. **33**, 14 (2000).
5. A. Poves, J. Sánchez-Solano, E. Caurier, F. Nowacki, Nucl. Phys. A **694**, 157 (2001).
6. A. Poves, A.P. Zuker, Phys. Rep. **70**, 235 (1981).
7. Data extracted using the NNDC WorldWideWeb site from the ENSDF database.
8. P.F. Mantica *et al.*, Phys. Rev. C **67**, 014311 (2003).
9. R.V.F. Janssens *et al.*, Phys. Lett. B **546**, 55 (2002).
10. S.N. Liddick *et al.*, Phys. Rev. Lett. **92**, 072502 (2004).
11. T. Otsuka *et al.*, Phys. Rev. Lett. **87**, 082502 (2001).
12. W.A. Richter, M.G. van der Merwe, R.E. Julies, B.A. Brown, Nucl. Phys. A **523**, 325 (1991).
13. B. Fornal, private communication.
14. M. Honma, B.A. Brown, T. Mizusaki, T. Otsuka, Nucl. Phys. A **704**, 134c (2002).
15. T. Otsuka, in preparation.
16. S.J. Freeman *et al.*, Phys. Rev. C **69**, 064301 (2004).
17. P.F. Mantica *et al.*, Phys. Rev. C **68**, 044311 (2003).
18. T.W. Burrows, Nucl. Data Sheets **76**, 191 (1995).